J. Fluid Mech. (2000), *vol.* 420, *pp.* 131–145. Printed in the United Kingdom

Structural instability of the bifurcation diagram for two-dimensional flow in a channel with a sudden expansion

By J. MIZUSHIMA AND Y. SHIOTANI

Department of Mechanical Engineering, Doshisha University, Kyotanabe, Kyoto 610-0321, Japan

(Received 31 August 1999 and in revised form 1 February 2000)

Flow in a symmetric channel with a sudden expansion makes a transition from a symmetric flow to an asymmetric one due to a symmetry-breaking pitchfork bifurcation on a gradual increase of the Reynolds number if the system is perfectly symmetric. However, an unavoidable infinitesimal imperfection of the system may render the pitchfork bifurcation imperfect. A weakly nonlinear stability analysis is proposed to investigate the structural instability of the bifurcation for such a flow. As a result, an amplitude equation for a disturbance is derived by including the effect of the imperfection of the system, and its coefficients are evaluated numerically. The equilibrium amplitude of the disturbance is calculated from the amplitude equation and compared with the experimental results for the flow in a channel that is presumed symmetric and also with the numerical solution of the full nonlinear equations for the flow in a slightly asymmetric channel.

1. Introduction

Two-dimensional flow in a symmetric channel with a sudden expansion is a typical example of a flow which is not homogeneous in its flow direction. Traditional stability theories for parallel flows cannot be applied to such a flow because of the inhomogeneity. So, the stability of the flow has been investigated mainly by numerical methods and experiments. It has been revealed that the transitions and instabilities of the flow include rich phenomena because of the inhomogeneity.

Durst, Melling & Whitelaw (1974) made detailed studies of the transition of two-dimensional flows in a presumed symmetric channel with a sudden expansion. They measured velocity profiles of the flow experimentally by LDV (laser Doppler velocimetry) and examined the flow patterns by flow visualization methods. The velocity profiles measured were in good agreement with those obtained by solving the two-dimensional momentum equation although the flow was strongly three-dimensional even well away from the channel corners, except at the lowest measurable velocities. They found that the flow is symmetric at low Reynolds numbers, but becomes asymmetric at higher Reynolds numbers. At very high Reynolds numbers the flow became periodic in time.

The phenomenon of the asymmetric separation of internal laminar flow in a channel with a sudden expansion was attributed to an instability of the shear layer by Cherdron, Durst & Whitelaw (1978), although this phenomenon had been explained by a 'Coanda' effect. They used flow visualization and LDV to clarify the mechanism

that yields the asymmetry and showed that the small disturbances generated at the lip of the sudden expansion are amplified in the shear layers which are formed between the main flow and the recirculation flow in the corners. But their explanation of the phenomenon was inadequate.

The origin of steady asymmetric flows in a symmetric sudden expansion was clarified by Fearn, Mullin & Cliffe (1990) by using experimental and numerical techniques. They showed that the asymmetry arises at a critical Reynolds number due to a pitchfork bifurcation and evaluated the critical Reynolds number. The experimentally measured degree of asymmetry at each value of Re showed a satisfactory agreement with the corresponding value obtained from the numerical results except in the immediate vicinity of the bifurcation, but the experimental bifurcation diagram is disconnected owing to small imperfections that are inevitably present in the experimental apparatus. Thus, there was no experimentally observed critical value of the Reynolds number and no perfectly symmetric state. So, they made an attempt to model numerically the effect of small imperfections in the flow channel, in order to try to account for the disconnection in the experimental bifurcation diagram. They made numerical calculations of the flow in a very slightly asymmetric channel, where the whole downstream section of the grid was shifted up by 1.25% of the width of the inlet channel with respect to the axis of symmetry. The numerical results showed that the size of the disconnection is of the same order as the size of decoupling found experimentally. They also observed time-dependent flows at higher Reynolds numbers and attributed the appearance of the unsteadiness to three-dimensional effects.

The linear stability of steady flows in a symmetric channel with a sudden expansion was determined by an Arnoldi-based iterative method for calculating the most unstable eigenmodes by Alleborn *et al.* (1997). They also applied a continuation method to study the bifurcation structure of the steady-state solution of the flow, where the effect of the asymmetry of the channel was also considered. And they obtained complete bifurcation diagrams which include unstable branches as well as stable branches. The linear growth rate of the least-stable disturbance was also evaluated by Shapira, Degani & Weihs (1990), where a time-dependent finite element solver was used.

It is known that the weakly nonlinear stability theory may play an important role in explaining the origin of the imperfect pitchfork bifurcation and evaluating the magnitude of the disconnection of the bifurcation diagram. The imperfect pitchfork bifurcation arises through the structural instability of the pitchfork bifurcation due to an infinitesimal perturbation, i.e. an asymmetry of the channel, which can be represented by an amplitude equation, but the reduction method to derive the amplitude equation from the basic equations (Navier–Stokes and continuity equations) has not been established. The classical weakly nonlinear theory developed by Stuart and Watson is applicable only to parallel flows (see Drazin & Reid 1981). An attempt to formulate the weakly nonlinear stability theory for the flow in an expanded channel was made by Sobey & Drazin (1986). They derived an amplitude equation by assuming Jeffery–Hamel flow to be a good local approximation for the flow, but encountered the discrepancy that the amplitude equation shows a subcritical pitchfork bifurcation for Jeffery–Hamel flow, whereas it is known that the flow in an expanded channel undergoes a supercritical pitchfork bifurcation.

In the present paper, we propose a formulation to derive the amplitude equation by applying the weakly nonlinear stability method to the flow in a slightly asymmetric channel with a sudden expansion and also propose a numerical method to evaluate the coefficients of the amplitude equation, including the linear growth rate of the disturbance.

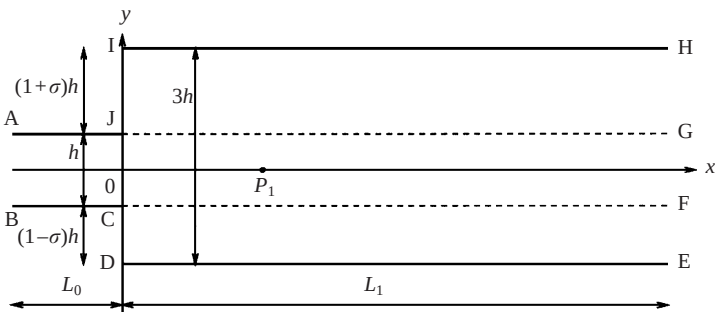

FIGURE 1. Configuration and coordinates.

2. Mathematical formulation

2.1. *Problem description and basic equations*

We consider an almost symmetric channel with a sudden expansion as shown in figure 1. Flow comes in from the inlet AB of width h, enters the expansion IDEH through the sudden expansion JC, and goes out from the outlet HE of width $3h$. The expansion ratio E is defined as $E = \mathrm{HE}/\mathrm{AB}$ and is fixed as $E = 3$ in the present study, for which case detailed experimental data are available to compare (Fearn *et al.* 1990). The centre-axis of the expanded channel IDEH is shifted up by σh with respect to the axis of the inlet channel ABCJ, and so the whole channel has an asymmetry due to the difference between the axes of the inlet and expanded channels. We call σ the asymmetry ratio hereafter. So, a channel with $\sigma = 0$ is symmetric along the x-axis.

We assume an incompressible and two-dimensional flow field; then the stream function $\psi(x, y, t)$ and the vorticity $\omega(x, y, t)$ formulation can be employed. The vorticity transport and Poisson equations are written in a non-dimensional form as

$$\frac{\partial \omega}{\partial t} = ReJ(\psi, \omega) + \Delta\omega, \tag{2.1}$$

$$\omega = -\Delta\psi, \tag{2.2}$$

where

$$\Delta \equiv \frac{\partial^2}{\partial x^2} + \frac{\partial^2}{\partial y^2}, \quad J(f, g) \equiv \frac{\partial f}{\partial x}\frac{\partial g}{\partial y} - \frac{\partial f}{\partial y}\frac{\partial g}{\partial x}.$$

All the variables are normalized by using the maximum inlet velocity $U_{\max}$ and the half-width $h/2$ of the inlet channel as representative velocity and length scales. It is noted that the time t is normalized by $\nu/U_{\max}^2$. The Reynolds number is defined as $Re = U_{\max}h/2\nu$. The set of equations (2.1) and (2.2) is written in an alternative form as

$$\mathrm{M}\frac{\partial \psi}{\partial t} = \mathrm{L}\psi + ReN(\psi, \psi), \tag{2.3}$$

where $\mathrm{M} \equiv \Delta$, $\mathrm{L} \equiv \Delta\Delta$ and $N(f, g) \equiv J(f, \Delta g)$.

The boundary condition at AB is assumed as a fully developed plane Poiseuille flow so that

$$\left.\begin{aligned} \frac{\partial \psi}{\partial x} = 0, \quad \frac{\partial \omega}{\partial x} = 0, \\ \psi = \int_{-1}^{y} u\mathrm{d}y = \int_{-1}^{y} (1 - y^2)\mathrm{d}y = y(1 - \tfrac{1}{3}y^2) + \tfrac{2}{3}. \end{aligned}\right\} \tag{2.4}$$

The outlet condition at HE is

$$\frac{\partial^2\psi}{\partial x^2} = 0, \quad \frac{\partial^2\omega}{\partial x^2} = 0, \tag{2.5}$$

because we consider only steady flows in the present paper; otherwise the Sommerfeld radiation condition may be appropriate.

The boundary conditions on all the walls are the non-slip condition, so the values of the stream function on the walls are determined as

$$\psi = \psi_1 = 0 \quad \text{on BCDE},$$

$$\psi = \psi_2 = \tfrac{4}{3} \quad \text{on AJIH},$$

$$\frac{\partial\psi}{\partial y} = 0 \quad \text{on (BC, DE, AJ, IH)}, \quad \frac{\partial\psi}{\partial x} = 0 \quad \text{on (CD, IJ)}, \tag{2.6}$$

because the volumetric flow rate in each cross-section of the channel is constant.

2.2. *Steady-state solution*

The flow in a symmetric channel ($\sigma = 0$) with a sudden expansion is steady and symmetric for small Reynolds numbers. The basic flow in the linear and weakly nonlinear stability analyses is steady symmetric flow in a symmetric channel. On the other hand, it is steady but asymmetric for the asymmetric channel ($\sigma \neq 0$) for small Reynolds numbers. The steady-state solution ($\bar{\psi}$, $\bar{\omega}$) satisfies the steady-state vorticity transport equation and the Poisson equation, which are obtained by dropping the time-derivative term in (2.3) as

$$\mathrm{L}\bar{\psi} + ReN(\bar{\psi}, \bar{\psi}) = 0. \tag{2.7}$$

Equation (2.7) is

$$Re\left(\frac{\partial\bar{\psi}}{\partial y}\frac{\partial\bar{\omega}}{\partial x} - \frac{\partial\bar{\psi}}{\partial x}\frac{\partial\bar{\omega}}{\partial y}\right) = \frac{\partial^2\bar{\omega}}{\partial x^2} + \frac{\partial^2\bar{\omega}}{\partial y^2}, \tag{2.8}$$

$$\bar{\omega} = -\left(\frac{\partial^2\bar{\psi}}{\partial x^2} + \frac{\partial^2\bar{\psi}}{\partial y^2}\right). \tag{2.9}$$

The steady-state solution is obtained by solving (2.8), (2.9) numerically by the SOR iterative method, or by solving (2.1), (2.2) by the time marching method. It is noted that the stream function $\bar{\psi}$ for a symmetric steady flow is anti-symmetric along the x-axis, i.e. the anti-symmetric stream function yields a symmetric flow field.

2.3. *Linear stability of the steady-state solutions*

The symmetric steady flow in a symmetric channel with a sudden expansion becomes unstable to small disturbances at a critical Reynolds number Re_c, and an asymmetric steady flow appears due to a pitchfork bifurcation as a result of the instability for $Re > Re_c$. We consider a disturbance (ψ', ω') added to the symmetric steady flow ($\bar{\psi}$, $\bar{\omega}$) to investigate its linear stability. Then the vorticity and the stream function are written as $\omega = \bar{\omega} + \bar{\omega}'$ and $\psi = \bar{\psi} + \psi'$. By substituting this expression for ψ into (2.3) and subtracting (2.7), we obtain an equation for ψ' as

$$\mathrm{M}\frac{\partial\psi'}{\partial t} = \mathrm{L}\psi' + ReN(\bar{\psi}, \psi') + ReN(\psi', \bar{\psi}) + ReN(\psi', \psi'). \tag{2.10}$$

We neglect the nonlinear term of ψ' in (2.10) and assume the time dependence of the disturbance as $\psi' = \hat{\psi}(x, y)\exp(\lambda t)$ and $\omega' = \hat{\omega}(x, y)\exp(\lambda t)$, where λ is the complex

linear growth rate of the disturbance. Then the linear stability equation is

$$\lambda \mathrm{M}\hat{\psi} = \mathrm{L}\hat{\psi} + ReN(\bar{\psi}, \hat{\psi}) + ReN(\hat{\psi}, \bar{\psi}). \tag{2.11}$$

Equation (2.11) is rewritten as

$$\lambda\hat{\omega} = \frac{\partial^2\hat{\omega}}{\partial x^2} + \frac{\partial^2\hat{\omega}}{\partial y^2} + Re\left(\frac{\partial\bar{\psi}}{\partial x}\frac{\partial\hat{\omega}}{\partial y} - \frac{\partial\bar{\psi}}{\partial y}\frac{\partial\hat{\omega}}{\partial x} + \frac{\partial\hat{\psi}}{\partial x}\frac{\partial\bar{\omega}}{\partial y} - \frac{\partial\hat{\psi}}{\partial y}\frac{\partial\bar{\omega}}{\partial x}\right), \tag{2.12}$$

$$\hat{\omega} = -\left(\frac{\partial^2\hat{\psi}}{\partial x^2} + \frac{\partial^2\hat{\psi}}{\partial y^2}\right). \tag{2.13}$$

The boundary conditions for $(\hat{\psi}, \hat{\omega})$ are

$$\left.\begin{aligned} \hat{\psi} = 0, \quad \frac{\partial\hat{\psi}}{\partial x} = 0, \quad \frac{\partial\hat{\omega}}{\partial x} = 0 \quad \text{on AB}, \\ \frac{\partial^2\hat{\psi}}{\partial x^2} = 0, \quad \frac{\partial^2\hat{\omega}}{\partial x^2} = 0 \quad \text{on HE}, \\ \hat{\psi} = 0, \quad \frac{\partial\hat{\psi}}{\partial y} = 0 \quad \text{on (BC, DE, AJ, IH)}, \quad \hat{\psi} = 0, \quad \frac{\partial\hat{\psi}}{\partial x} = 0 \quad \text{on (CD, IJ)}. \end{aligned}\right\} \tag{2.14}$$

The value of λ is found by solving (2.12), (2.13) under the boundary condition (2.14) with the SOR iterative method. The real part of λ, say λ_r, indicates the linear growth rate of the disturbance. The steady symmetric flow is unstable if $\lambda_r > 0$, or stable if $\lambda_r < 0$. The Reynolds number Re_c at which $\lambda_r = 0$ gives the critical Reynolds number Re_c. It is shown that the imaginary part of λ, λ_i, is zero, which shows that the exchange of stability is valid for the present problem. And the eigenfunctions $(\hat{\psi}, \hat{\omega})$ at the critical state are shown to be real functions. It is noted that the eigenfunction $\hat{\psi}$ for the most unstable mode is symmetric along the x-axis, i.e. the flow field of the disturbance is anti-symmetric.

2.4. *Weakly nonlinear stability analysis for the imperfect pitchfork bifurcation*

We consider the weakly nonlinear behaviour of the disturbance added to the symmetric flow near the critical state ($Re = Re_c$) and evaluate the effect of the slight asymmetry of the channel by the weakly nonlinear stability analysis. We derive an amplitude equation to account for the imperfect pitchfork bifurcation.

We begin with (2.3) and transform the variable y as $\eta = (y - \delta)/(1 + \delta\sigma) + \delta$, where $\delta = +1$ in IJGH, $\delta = -1$ in CDEF, and $\delta = 0$ in ABFG of figure 1. Then, the asymmetric channel is transformed to an apparently symmetric channel, but the operators are modified as

$$\left.\begin{aligned} \frac{\partial}{\partial y} = \frac{1}{1+\delta\sigma}\frac{\partial}{\partial\eta} \simeq (1-\delta\sigma)\frac{\partial}{\partial\eta}, \\ \Delta = \frac{\partial^2}{\partial x^2} + \frac{\partial^2}{\partial y^2} \simeq \frac{\partial^2}{\partial x^2} + (1-\delta\sigma)^2\frac{\partial^2}{\partial\eta^2} \simeq \frac{\partial^2}{\partial x^2} + \frac{\partial^2}{\partial\eta^2} - 2\delta\sigma\frac{\partial^2}{\partial\eta^2}, \end{aligned}\right\} \tag{2.15}$$

$$\begin{aligned} \Delta^2 &= \left(\frac{\partial^2}{\partial x^2} + \frac{\partial^2}{\partial y^2}\right)\left(\frac{\partial^2}{\partial x^2} + \frac{\partial^2}{\partial y^2}\right) \\ &\simeq \frac{\partial^4}{\partial x^4} + 2\frac{\partial^2}{\partial x^2}\frac{\partial^2}{\partial\eta^2} + \frac{\partial^4}{\partial\eta^4} - 4\delta\sigma\left(\frac{\partial^2}{\partial x^2}\frac{\partial^2}{\partial\eta^2} + \frac{\partial^4}{\partial\eta^4}\right), \end{aligned} \tag{2.16}$$

where we have omitted terms of higher order than $O(\sigma)$ by considering the asymmetry parameter σ very small. We must be careful in evaluating η-derivatives by finite

difference approximations along JG and CF (figure 1). Equation (2.3) is written in the new variable η as

$$\frac{\partial}{\partial t}(\mathrm{M}_0 - \delta\sigma \mathrm{M}_1)\psi = ReN_0(\psi,\ \psi) - \delta\sigma ReN_1(\psi,\ \psi) + \mathrm{L}_0\psi - \delta\sigma \mathrm{L}_1\psi, \tag{2.17}$$

where

$$\left.\begin{gathered} \mathrm{M}_0 = \Delta_\eta, \quad \mathrm{M}_1 = 2\frac{\partial^2}{\partial\eta^2}, \quad \mathrm{L}_0 = \Delta_\eta\Delta_\eta, \quad \mathrm{L}_1 = 4\Delta_\eta\frac{\partial^2}{\partial\eta^2}, \\ N_0(f,\ g) = J(f,\ \Delta_\eta g), \quad N_1(f,\ g) = J(f,\ \mathrm{D}^2 g), \\ \Delta_\eta = \frac{\partial^2}{\partial x^2} + \frac{\partial^2}{\partial\eta^2}, \quad \mathrm{L}^2 = \frac{\partial^2}{\partial x^2} + 3\frac{\partial^2}{\partial\eta^2}. \end{gathered}\right\} \tag{2.18}$$

We express the stream function ψ as the sum of the steady-state solution $\bar{\psi}(x, y)$ and the disturbance $\psi'(x, y, t)$ as $\psi = \bar{\psi} + \psi'$. Substituting this expression for ψ into (2.17) and subtracting (2.7), we obtain an equation for ψ' as

$$\begin{aligned} \frac{\partial}{\partial t}(\mathrm{M}_0 - \delta\sigma \mathrm{M}_1)\psi' = {} & \mathrm{L}_0\psi' - \delta\sigma \mathrm{L}_1\psi' + ReN_0(\bar{\psi},\ \psi') + ReN_0(\psi', \bar{\psi}) + ReN_0(\psi', \psi') \\ & - \delta\sigma ReN_1(\bar{\psi}, \bar{\psi}) - \delta\sigma ReN_1(\bar{\psi}, \psi') - \delta\sigma ReN_1(\psi', \bar{\psi}) - \delta\sigma ReN_1(\psi', \psi'). \end{aligned} \tag{2.19}$$

For the local bifurcation analysis near the critical state ($Re \gtrsim Re_\mathrm{c}$), we adopt ϵ, defined by $\epsilon^2 \equiv Re - Re_\mathrm{c}$, as a small parameter and put $\sigma = \epsilon^3\sigma_1$ by assuming the asymmetry σ of the channel is very small as $\sigma \sim O(\epsilon^3)$, which is the smallest magnitude to be included in the lowest-order analysis ($O(\epsilon^3)$) of the pitchfork bifurcation. We expand physical quantities such as $\bar{\psi}$, ψ' and t in ϵ as

$$\left.\begin{aligned} \psi' &= \epsilon\tilde{\psi}_1 + \epsilon^2\tilde{\psi}_2 + \epsilon^3\tilde{\psi}_3 + \cdots, \\ \bar{\psi} &= \bar{\psi}_0 + \epsilon^2\bar{\psi}_1 + \cdots, \\ \frac{\partial}{\partial t} &= \frac{\partial}{\partial t_0} + \epsilon^2\frac{\partial}{\partial t_1} + \cdots. \end{aligned}\right\} \tag{2.20}$$

The expansion of $\bar{\psi}$ comes from the fact that $\bar{\psi}$ is a function of Re, so $\bar{\psi} = \bar{\psi}_0 + (Re - Re_\mathrm{c})(\partial\bar{\psi}/\partial Re)_{Re=Re_\mathrm{c}} + \cdots$. The expansions of ψ' and t are similar to those in the conventional weakly nonlinear stability analysis for parallel flows.

The equations for $\bar{\psi}_0$ and $\bar{\psi}_1$ are obtained by substituting the expansion of $\bar{\psi}$ into (2.7) and equating terms of the same order, $O(1)$ and $O(\epsilon^2)$, respectively. The equation for $\bar{\psi}_0$ has the same form as (2.7) with Re being replaced by Re_c and is expressed as

$$\mathrm{L}\bar{\psi}_0 + Re_\mathrm{c}N(\bar{\psi}_0, \bar{\psi}_0) = 0. \tag{2.21}$$

The function $\bar{\psi}_1$ is the derivative of $\bar{\psi}$ with respect to Re at Re_c, expressed as $(\partial\bar{\psi}/\partial Re)|_{Re=Re_\mathrm{c}}$ and satisfies the equation

$$\mathrm{L}\bar{\psi}_1 + N(\bar{\psi}_0, \bar{\psi}_0) + Re_\mathrm{c}N(\bar{\psi}_1, \bar{\psi}_0) + Re_\mathrm{c}N(\bar{\psi}_0, \bar{\psi}_1) = 0. \tag{2.22}$$

The symmetric steady-state solution $\bar{\psi}_0$ must satisfy the boundary conditions (2.4), (2.5) and (2.6), whereas the boundary conditions for $\bar{\psi}_1$ are the same as those for $\hat{\psi}$, i.e. (2.14). The functions $\bar{\psi}_0$ and $\bar{\psi}_1$ are obtained by solving (2.21) and (2.22) numerically under the boundary conditions (2.4), (2.5), (2.6) and (2.14) with the SOR iterative method, respectively.

The equations for $\tilde{\psi}_1$, $\tilde{\psi}_2$ and $\tilde{\psi}_3$ are obtained by substituting the expansion of $\tilde{\psi}$ into (2.19) and equating terms of the same order, $O(\epsilon)$, and $O(\epsilon^2)$ and $O(\epsilon^3)$,

respectively. The equation for $\tilde{\psi}_1$ is expressed as

$$\mathrm{L}_0\tilde{\psi}_1 + Re_c N_0(\bar{\psi}_0, \tilde{\psi}_1) + Re_c N_0(\tilde{\psi}_1, \bar{\psi}_0) = 0, \tag{2.23}$$

which is identical to (2.11) if it is considered that the complex linear growth rate λ is identically zero at the critical state.

The boundary conditions for $\tilde{\psi}_1$ should be the same as those for ψ', but we choose modified boundary conditions rather than (2.14) for the sake of simplicity to define an adjoint function of $\tilde{\psi}_1$, which are expressed as

$$\left.\begin{gathered} \tilde{\psi}_1 = 0, \quad \frac{\partial \tilde{\psi}_1}{\partial x} = 0 \text{ on (AB, HE)}, \\ \tilde{\psi}_1 = 0, \quad \frac{\partial \tilde{\psi}_1}{\partial y} = 0 \text{ on (BC, DE, AJ, IH)}, \quad \tilde{\psi}_1 = 0, \quad \frac{\partial \tilde{\psi}_1}{\partial x} = 0 \text{ on (CD, IJ).} \end{gathered}\right\} \tag{2.24}$$

It is confirmed by numerical calculations of (2.23) under the two different boundary conditions (2.14) and (2.24) that modification of the boundary condition does not affect the eigenfunction $\tilde{\psi}_1$ significantly. This is because the disturbance $\tilde{\psi}_1$ has no significant magnitude as far downstream as the outlet HE. In other words, the bifurcated flow becomes fully developed plane Poiseiulle flow near the outlet HE. This is in contrast with the case of the Hopf bifurcation, where the disturbance travels far downstream as Tollmien–Schlichting waves.

Since equation (2.23) is linear and homogeneous, we need to impose an additional condition, i.e. a normalization condition, to determine the solution uniquely. In the normalization of $\tilde{\psi}_1$, we adopt the velocity v_1 in the y-direction at a representative point $\mathrm{P}_1 = (x_1, \eta_1) = (12.75, 0)$ as the representative quantity which manifests the magnitude of the asymmetry of the flow (see figure 1). Then the solution $\tilde{\psi}_1$ is obtained by solving (2.23) under the boundary condition (2.24) with the SOR iterative method in the form

$$\tilde{\psi}_1 = A(t) g_1(x, \eta) \tag{2.25}$$

with the normalization condition $-\partial g_1/\partial x(x_1, \eta_1) = 1$. With this normalization, we can consider the amplitude $A(t)$ as the magnitude of the velocity v_1 in the y-direction at P_1. It is shown that the eigenfunction g_1 is symmetric along the x-axis.

The adjoint equation of (2.23) is

$$\mathrm{L}_0\tilde{g} - Re_c N_0(\bar{\psi}_0, \tilde{g}) - Re_c N_2(\bar{\psi}_0, \tilde{g}) + Re_c N_2(\tilde{g}, \bar{\psi}_0) = 0, \tag{2.26}$$

where

$$N_2(f, g) = 2\frac{\partial^2 f}{\partial x \partial y}\left(\frac{\partial^2 g}{\partial x^2} - \frac{\partial^2 g}{\partial y^2}\right).$$

The function $\tilde{g}$ is an adjoint function of g_1 which satisfies the same boundary conditions (2.24) as those for g_1. Needless to say the adjoint function is also symmetric along the x-axis.

The equation for $\tilde{\psi}_2$ is obtained by collecting $O(\epsilon^2)$ terms as

$$\mathrm{L}_0\tilde{\psi}_2 + Re_c N_0(\bar{\psi}_0, \tilde{\psi}_2) + Re_c N_0(\tilde{\psi}_2, \bar{\psi}_0) + Re_c N_0(\tilde{\psi}_1, \tilde{\psi}_1) = 0. \tag{2.27}$$

The boundary conditions for $\tilde{\psi}_2$ are the same as those for g_1, but the function $\tilde{\psi}_2$ is anti-symmetric along the x-axis. The equation (2.27) is linear but inhomogeneous, so the solution $\tilde{\psi}_2$ is obtained without any normalization condition and is written as

$$\tilde{\psi}_2 = A(t)^2 g_2(x, \eta) + C g_1(x, \eta). \tag{2.28}$$

The coefficient C in (2.28) is determined as $C = 0$ from symmetry considerations.

By collecting the terms of $O(\epsilon^3)$, we obtain the equation for $\tilde{\psi}_3$ as

$$\begin{aligned}&\mathrm{L}_0\tilde{\psi}_3 + Re_c N_0(\bar{\psi}_0, \tilde{\psi}_3) + Re_c N_0(\tilde{\psi}_3, \bar{\psi}_0)\\ &\quad = \frac{\partial}{\partial t_1}\mathrm{M}_0\tilde{\psi}_1 - Re_c N_0(\bar{\psi}_1, \tilde{\psi}_1) - N_0(\bar{\psi}_0, \tilde{\psi}_1) - Re_c N_0(\tilde{\psi}_1, \bar{\psi}_1) - N_0(\tilde{\psi}_1, \bar{\psi}_0)\\ &\qquad -Re_c N_0(\tilde{\psi}_1, \tilde{\psi}_2) - Re_c N_0(\tilde{\psi}_2,\ \tilde{\psi}_1) + \delta\sigma_1 Re_c N_1(\bar{\psi}_0, \bar{\psi}_0) + \delta\sigma_1 L_1\bar{\psi}_0. \qquad (2.29)\end{aligned}$$

Equation (2.29) has a solution if and only if the solvability condition

$$\begin{aligned}\int_D \tilde{g}\Big\{ &\frac{\partial}{\partial t_1}\mathrm{M}_0\tilde{\psi}_1 - Re_c N_0(\bar{\psi}_1, \tilde{\psi}_1) - N_0(\bar{\psi}_0,\ \tilde{\psi}_1)\\ &-Re_c N_0(\tilde{\psi}_1, \bar{\psi}_1) - N_0(\tilde{\psi}_1,\ \bar{\psi}_0) - Re_c N_0(\tilde{\psi}_1, \tilde{\psi}_2) - Re_c N_0(\tilde{\psi}_2,\ \tilde{\psi}_1)\\ &+\delta\sigma_1 Re_c N_1(\bar{\psi}_0, \bar{\psi}_0) + \delta\sigma_1 \mathrm{L}_1\bar{\psi}_0\Big\}\mathrm{d}x\mathrm{d}y = 0 \qquad (2.30)\end{aligned}$$

is satisfied, where D is the domain ABCDEHIJ in figure 1. On substitution of (2.25) and (2.28), equation (2.30) leads to an amplitude equation

$$\frac{\mathrm{d}A}{\mathrm{d}t_1} = \lambda_1 A + \lambda_2 A^3 + \lambda_0\sigma_1, \qquad (2.31)$$

where

$$\lambda_1 = \frac{\alpha_1}{\beta}, \quad \lambda_2 = \frac{\alpha_2}{\beta}, \quad \lambda_0 = \frac{\alpha_0}{\beta}, \qquad (2.32)$$

$$\beta = \int_D \tilde{g}\mathrm{M}_0 g_1 \mathrm{d}x\mathrm{d}y, \qquad (2.33)$$

$$\alpha_1 = \int_D \tilde{g}\{Re_c N_0(\bar{\psi}_1, g_1) + N_0(\bar{\psi}_0, g_1) + Re_c N_0(g_1, \bar{\psi}_1) + N_0(g_1, \bar{\psi}_0)\}\mathrm{d}x\mathrm{d}y, \qquad (2.34)$$

$$\alpha_2 = \int_D \tilde{g}\{Re_c N_0(g_1, g_2) + Re_c N_0(g_2, g_1)\}\mathrm{d}x\mathrm{d}y, \qquad (2.35)$$

$$\alpha_0 = -\int_D \tilde{g}\{\delta Re_c N_1(\bar{\psi}_0, \bar{\psi}_0) + \delta L_1\bar{\psi}_0\}\mathrm{d}x\mathrm{d}y. \qquad (2.36)$$

The integrations in (2.33)–(2.36) are evaluated numerically by Simpson's formula.

Equation (2.31) can be rewritten in original variables as

$$\frac{\mathrm{d}v_1}{\mathrm{d}t} = \lambda_1(Re - Re_c)v_1 + \lambda_2 {v_1}^3 + \sigma\lambda_0, \qquad (2.37)$$

where relations

$$\epsilon^2 = (Re - Re_c), \quad \epsilon^2\frac{\partial}{\partial t_1} = \frac{\partial}{\partial t}, \quad \epsilon A = v_1$$

are utilized.

2.5. *Numerical methods*

We have performed numerical simulations for the flow in a channel with a sudden expansion by the time marching method. The whole computational domain is discretized by an equally spaced mesh with $\Delta x = \Delta y = 0.1$. The vorticity transport equation (2.1) is approximated by the explicit Euler method with first-order accuracy in time together with second-order accuracy of central finite differences in space. The time increment Δt is chosen as $\Delta t = 0.001$ or $\Delta t = 0.0005$ depending upon the Reynolds number. The Poisson equation (2.2) is approximated by second-order central finite

differences and solved by the SOR method, where the relaxation factor $r = 1.5$ is used. The convergence of the SOR method is determined when the maximum relative error for the stream function reaches 10^{-5} and the steady flow state is determined when the stream function becomes time independent and the maximum relative error reaches 10^{-10}.

The steady-state solutions are also obtained numerically from the steady-state equations. Both the steady-state vorticity transport equation obtained by putting $\mathrm{d}/\mathrm{d}t = 0$ in (2.4) and the Poisson equation (2.5) are solved by the SOR iterative method. Finite difference approximations in an equally spaced mesh with $\Delta x = \Delta y = 0.1$ are used. Spatial derivatives are approximated by fourth-order finite differences. The relaxation factor r for the SOR method is in the range $0.7 < r < 1.0$ depending upon the Reynolds number. The convergence of the SOR method is determined when the maximum relative error for the stream function reaches 10^{-10}. In order to calculate unstable steady symmetric solutions above a critical Reynolds number, the SOR method is utilized under the symmetry condition along the centreline of the channel. The eigenvalue problem for the linear stability equations (2.12) and (2.13) is also solved by the SOR method in a similar way to the steady-state solutions except that λ is also assumed as a dependent variable as well as $\hat{\psi}$ and one more equation $-(\partial\hat{\psi}/\partial x)_{\mathrm{P}_1} = 1$ (figure 1), i.e. the normalization condition, is solved besides (2.12) and (2.13).

3. Numerical results

3.1. *Transition of the flow*

It is confirmed by our numerical simulations that the flow in a symmetric channel with a sudden expansion ($\sigma = 0$) approaches a unique steady state after enough time has elapsed at low Reynolds numbers. The flow pattern is symmetric along the centre of the channel as shown in figure 2(*a*), where streamlines of the flow are depicted for $Re = 40$ as a typical example. It is seen in this figure that the flow field has two recirculation vortices with equal lengths behind the backward facing steps. As the Reynolds number is increased, the symmetric flow becomes unstable at a critical Reynolds number Re_{c} and an asymmetric flow appears due to a symmetry-breaking pitchfork bifurcation for $Re > Re_{\mathrm{c}}$. Figure 2(*b*) shows the flow pattern of such an asymmetric flow at $Re = 45$. We can see in this figure that the flow bends towards one sidewall behind the sudden expansion. The direction of the bend is determined randomly with equal probabilities for the two directions theoretically, although it is determined by the algorithm in the computation. The sizes of the two recirculation vortices are quite different from each other.

We have calculated the equilibrium solution with the SOR method to confirm the bifurcation phenomena obtained by Fearn *et al.* (1990). We choose the velocity v_1 in the y-direction at $\mathrm{P}_1 = (x_1,\ \eta_1) = (12.75, 0)$ as the representative quantity which manifests the magnitude of the asymmetry as in the paper of Fearn *et al.* (1990). The bifurcation diagram is shown in figure 3, where the *dashed* lines show the values of v_1 for the stable asymmetric equilibrium solutions obtained by the SOR method and the *dotted* line indicates the unstable symmetric solution. We can see that the symmetric flow becomes unstable at $Re_{\mathrm{c}} = 40.23$ (P in figure 3), from which two asymmetric flows appear due to a symmetry-breaking pitchfork bifurcation. The bifurcation diagram obtained by Fearn *et al.* (1990) is depicted by a dash-dotted line in figure 3, which coincides with our numerical result (dashed line). Fearn *et al.* (1990) evaluated the

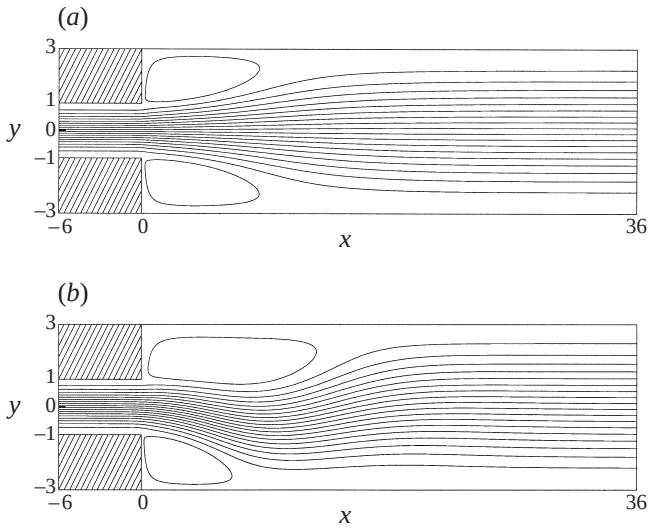

FIGURE 2. Flow patterns. $\sigma = 0$ (symmetric channel). (*a*) $Re = 40$, steady symmetric flow. (*b*) $Re = 45$, steady asymmetric flow.

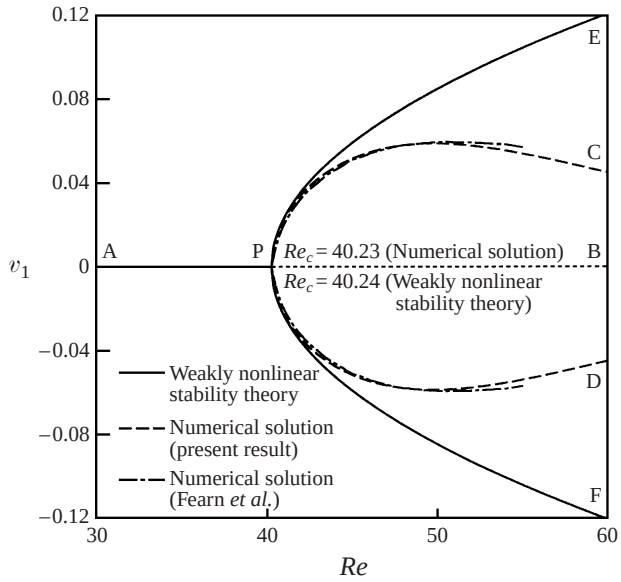

FIGURE 3. Bifurcation diagram. $\sigma = 0$ (symmetric channel).

critical Reynolds number as $Re_c = 40.45 \pm 0.17\%$, which should be compared with our estimation $Re_c = 40.23$. Note that the critical values Re_c have been obtained as $Re_c = 109$, 40, 21.4, 12.8 for $E = 2$, 3, 5, 10, respectively by Alleborn *et al.* (1997). And it is expected that Re_c tends to infinity as $E \to 1$.

3.2. *Linear growth rate*

We evaluate the linear growth rate of the symmetric flow in the symmetric channel ($\sigma = 0$), which is indicated by AB in figure 3, by solving (2.12), (2.13) under the boundary condition (2.14) by the SOR method with the finite difference approximation

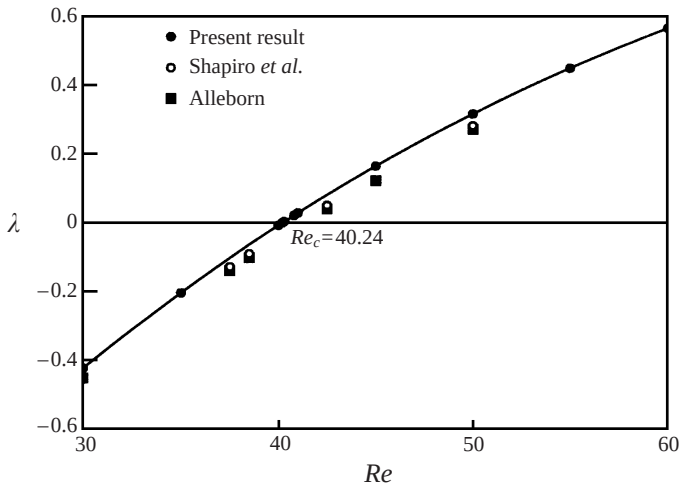

FIGURE 4. Linear growth rate λ for the steady symmetric flow (APB in figure 3). $\sigma = 0$ (symmetric channel).

in a similar way to obtain the steady-state solutions. In the numerical calculation of the linear growth rate, we have imposed the normalization condition that the velocity v_1 in the y-direction at $P_1 = (x_1, \eta_1) = (12.75, 0)$ is unity. The normalization condition is not essential in the evaluation of the linear growth rate, but is important for the convergence of the SOR iterative method. The complex growth rate is shown to be real ($\lambda_i = 0$), that is, the exchange of stability is proved to be valid in this case. The linear growth rates obtained are shown by filled circles in figure 4, where numerical data obtained by Alleborn (1999, personal communication) and Shapira *et al.* (1990) are also plotted (their values of λ', Re' are rescaled as $\lambda = Re\lambda'/2$, $Re = Re'/2$ to match the two different normalizations for time and length scales). The critical Reynolds number at which the linear growth rate becomes zero is evaluated as $Re_c = 40.24$, which is in good agreement with our numerical result ($Re_c = 40.23$) of the nonlinear equilibrium solution by the SOR method. So it is concluded that the branch AP of the symmetric flow is stable, whereas the branch PB is unstable. Note also that the asymmetric solutions indicated by PC and PD are stable although we have not evaluated the linear growth rate for these solutions.

The flow pattern of the most unstable mode of disturbance at the critical Reynolds number $Re_c = 40.24$ is shown in figure 5, where the streamlines of the disturbance are depicted. It is seen that the disturbance has one vortex just behind the sudden expansion and that the vortex has a length of about $18h$ in the streamwise direction. The rather short length of the vortex is characteristic of the disturbance for symmetry-breaking pitchfork bifurcations. So, the bending part of the asymmetric flow resultant from the pitchfork bifurcation is limited to a finite region behind the sudden expansion of the channel.

Needless to say the difference of the asymmetric flows indicated by PC or PD in figure 3 from the symmetric flow PB has a similar flow pattern to the disturbance shown in figure 5, near the critical point P.

3.3. *Weakly nonlinear stability analysis*

It is known that the symmetric flow becomes unstable at the critical Reynolds number Re_c due to the symmetry-breaking pitchfork bifurcation for the case of symmetric

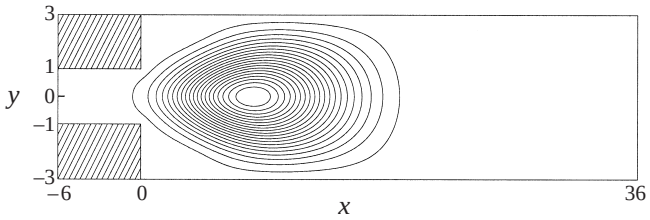

FIGURE 5. Flow pattern of the most unstable mode of disturbance at the critical Reynolds number ($Re_c = 40.24$).

channel ($\sigma = 0$). We have confirmed from our numerical results for the equilibrium solution that a relation $v_1^2 \propto (Re - Re_c)$ holds near the critical state, which shows that a pitchfork bifurcation occurs at the critical state. On the other hand, the amplitude equation (2.31) directly expresses the pitchfork bifurcation at the critical state.

We evaluate the coefficients λ_0, λ_1, λ_2 of the amplitude equation numerically and compare the amplitude evaluated from (2.31) with the numerical results of the equilibrium solution. For the evaluation of the coefficients, we need the functions $\bar{\psi}_0$, $\bar{\psi}_1$ for the steady-state solutions, and g_1, g_2, $\tilde{g}$ for the disturbance. The steady-state solutions $\bar{\psi}_0$ and $\bar{\psi}_1$ are obtained by solving (2.21) and (2.22) under the appropriate boundary conditions by the SOR iterative method in a similar way to the numerical calculations of the steady-state solution explained in § 2.5. The linear eigenfunction g_1 and its adjoint function $\tilde{g}$ are calculated by solving (2.23) and (2.26) under the boundary condition (2.24) by the SOR iterative method together with the normalization condition $v_1 = 1$ at $P_1 = (x_1, \eta_1)$. The function g_2 is calculated from (2.27) under the boundary condition (2.24) by assuming the anti-symmetric solution. The integrations in (2.33)–(2.36) are evaluated numerically with Simpson's formula. We adopt the value of $Re_c = 40.24$ as the critical Reynolds number, which is obtained by the linear stability theory. Thus the coefficients of the amplitude equation (2.31) are evaluated as $\lambda_1 = 3.6405 \times 10^{-2}$, $\lambda_2 = -4.9579 \times 10^{1}$, $\lambda_0 = 1.0404 \times 10^{-1}$.

For the case of a symmetric channel ($\sigma = 0$), the equilibrium amplitude v_1 is evaluated from (2.37) as

$$v_1 = \sqrt{-\frac{\lambda_1 (Re - Re_c)}{\lambda_2}}, \tag{3.1}$$

and the values of v_1 are plotted in figure 3. It is seen in figure 3 that the coinciding of the results of the weakly nonlinear stability analysis (solid line, EPF) and the numerical calculation of the equilibrium solution (dashed line, CPD) is limited to the vicinity of the critical point such that $Re_c = 40.24 \leqslant Re \lesssim 42$. However, it is thus proved by the weakly nonlinear stability analysis that a supercritical pitchfork bifurcation occurs at the critical point. So, the weakly nonlinear stability theory is a very powerful tool to help understand the phenomena underlying physics of the instability although its applicable parameter range is rather limited.

As an example of slightly asymmetric channel ($\sigma \neq 0$), we show the bifurcation diagram for $\sigma = 0.001$ in figure 6, where the velocity v_1 evaluated from (2.37) is depicted by solid and dotted lines. The solid line indicates the stable solution and the dotted line the unstable solution. The symbol T in figure 6 shows the turning point. Numerical results are also plotted by the dashed lines. Note that we could not calculate the unstable portion of the bifurcation diagram numerically. We can see

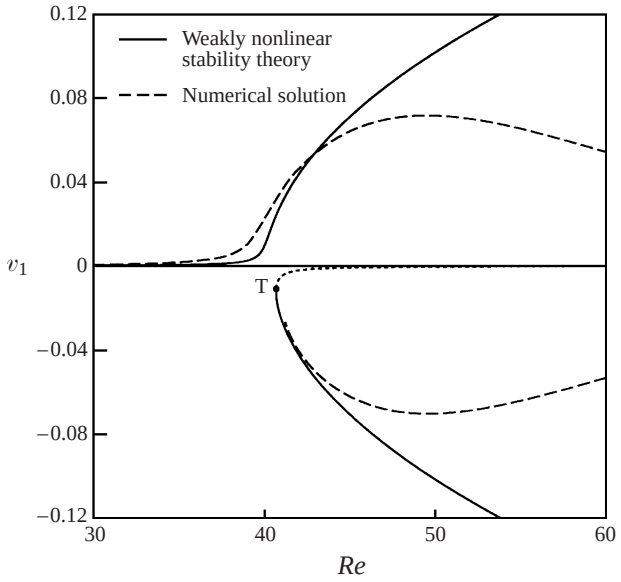

FIGURE 6. Bifurcation diagram. $\sigma = 0.001$ (asymmetric channel).

that the pitchfork bifurcation becomes imperfect even for a very slightly asymmetric channel. The amplitude v_1 evaluated by the weakly nonlinear stability analysis is in good accordance with the numerical results in quite a wide range of parameter *Re*.

As stated in the introduction, Fearn *et al.* investigated the transition of the flow in what they presumed to be a symmetric channel with a sudden expansion experimentally, and found that their experimental results did not agree with their numerical results. They compared the experimental results with the numerical ones for the flow in a slightly asymmetric channel with $\sigma = 0.0125$ by making the conjecture that an imperfection in their experimental apparatus may make the bifurcation imperfect, and obtained close agreement between experimental and numerical results. We also evaluate the equilibrium amplitude v_1 for $\sigma = 0.0125$ by the weakly nonlinear analysis from (2.37) and plot the values in figure 7. The solid lines indicate v_1 evaluated from the weakly nonlinear stability theory, the dashed lines the numerical solutions for $\sigma = 0.0125$, whereas the '+' symbols show the experimental results for the presumed symmetric channel by Fearn *et al.* (1990). It is seen in figure 7 that the weakly nonlinear stability analysis (solid line) and the numerical solution (dashed line) are in close agreement with the experimental results by Fearn *et al.* (1990) for the smooth transition branch in the upper half of the figure ($v_1 > 0$), but the coinciding of the solid and dashed lines with the symbols + (experiments) is not very good for the saddle node branch in the lower half of the figure ($v_1 < 0$). It is our speculation that the imperfection observed by Fearn *et al.* (1990) may partially come from the very slight asymmetry of the channel, but there may be other factors such as an asymmetry of the inlet flow and small thermal effects in the fluid. However, the inclusion of the asymmetry $\sigma = 0.0125$ of the channel gives better agreement with the experimental results than for the case of $\sigma = 0$ although the outlet as well as the inlet conditions in the numerical and laboratory experiments differ, especially for large values of the Reynolds number.

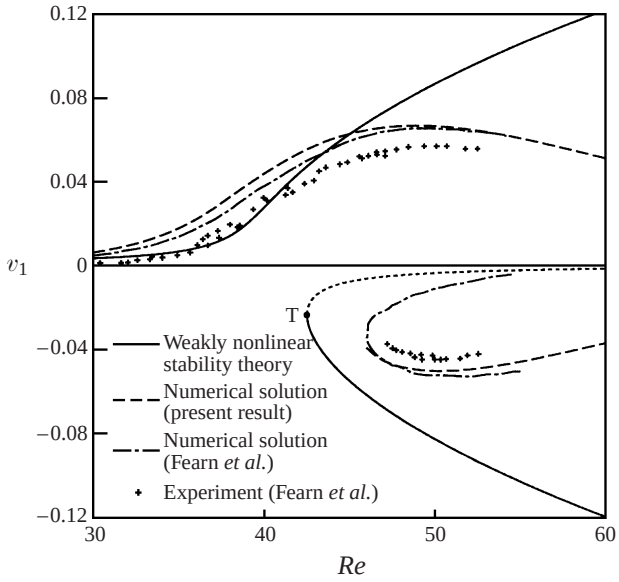

FIGURE 7. Bifurcation diagram. $\sigma = 0.0125$ (asymmetric channel).

4. Discussion

We have applied weakly nonlinear stability theory to the flow in a slightly asymmetric channel with a sudden expansion and evaluated the equilibrium amplitude from the amplitude equation. Experimental results are known to include the effect of a very small amount of imperfectness in the experimental apparatus, which makes the pitchfork bifurcation imperfect. We have estimated the magnitude of the imperfection σ in the experiments (Fearn *et al.* 1990) by fitting the value of v_1 evaluated from the weakly nonlinear stability theory with the experimental results. We obtained a value of $\sigma = 0.0125$ similar to Fearn *et al.* (1990) for the imperfection included in their experimental apparatus by the curve fitting.

We have compared the results from the weakly nonlinear stability analysis with the experimental and numerical results and shown that the parameter range where the weakly nonlinear stability theory gives a very good approximation is rather limited in the vicinity of the critical point. The unfolding of the pitchfork bifurcation due to an imperfection is familiar and the amplitude equation (2.37) is well known in dynamical system theory. Moreover the imperfect pitchfork bifurcation diagram has already been obtained experimentally. So, one might ask what is new in the present paper. Our answer is that the weakly nonlinear stability theory shows the essential and skeleton dynamics of the phenomena, from which we can understand the underlying physics of instabilities. It is this bridging of the gap between simple dynamical system theory and complex real fluid dynamics that is shown in the present analysis.

We have considered the perturbation (imperfection) to the system by considering there to be a difference in the axes of the inlet and expanded channels as well as in the disturbance to the basic symmetric flow, and evaluated the magnitude of the imperfection in the experimental apparatus. There may of course be other factors which render the pitchfork bifurcation imperfect. The effects of such factors can be considered in a similar way as the analysis in the present paper.

The authors express their cordial thanks to Professor H. Yamaguchi for valuable discussions. This work was partially supported by a Grant-in-Aid for Scientific Research (C) from Japan Society for the Promotion of Science and also by Doshisha University's Research Promotion Funds.

REFERENCES

Alleborn, N., Nandakumar, K., Raszillier, H. & Durst, F. 1997 Further contributions on the two-dimensional flow in a sudden expansion. *J. Fluid Mech.* **330**, 169–188.

Cherdron, W., Durst, F. & Whitelaw, J. H. 1978 Asymmetric flow and instabilities in symmetric ducts with sudden expansion. *J. Fluid Mech.* **84**, 13–31.

Drazin, P. G. & Reid, W. H. 1981 *Hydrodynamic Stability*, Chap. 7. Cambridge University Press.

Durst, F., Melling, A. & Whitelaw, J. H. 1974 Low Reynolds number flow over a plane symmetric sudden expansion. *J. Fluid Mech.* **64**, 111–128.

Fearn, R. M., Mullin, T. & Cliffe, K. A. 1990 Nonlinear flow phenomena in a symmetric sudden expansion. *J. Fluid Mech.* **211**, 595–608.

Shapira, M., Degani, D. & Weihs, D. 1990 Stability and existence of multiple solutions for viscous flow in suddenly enlarged channels. *Comput. Fluids* **18**, 239–258.

Sobey, I. J. & Drazin, P. G. 1986 Bifurcation of two-dimensional channel flows. *J. Fluid Mech.* **171**, 263–287.